Desalination and Water Treatment
www.deswater.com
doi: 10.5004/dwt.2021.27191

224 (2021) 421–432
June

Adsorptive removal of the azo dye Direct blue 2 onto agriculture waste corncob

Luis M. Gómez*, Angelina Hormaza

Research Group on Synthesis, Reactivity and Transformation of Organic Compounds – SIRYTCOR, School of Chemistry, Faculty of Science, Universidad Nacional de Colombia – Sede Medellín, Colombia, emails: lumgomezca@unal.edu.co (L.M. Gómez), ahormaza@unal.edu.co (A. Hormaza)

Received 19 December 2020; Accepted 19 February 2021

ABSTRACT

Lignocellulosic agricultural by-products have been used as non-conventional and inexpensive adsorbents for treating different pollutants. In this work, the uptake capacity of corncob (CC) was evaluated in the removal of Direct blue 2 (DB2) dye, a diazo dye widely used in the textile industry. A 2^3 full factorial design led to 88.3% DB2 removal under a CC dosage of 6.0 g L^{-1}, an initial DB2 concentration of 60 ppm, and a particle size range of 0.3–0.5 mm. A subsequent optimization of the process through a central composite surface design allowed to achieve an efficiency of 89.81% by increasing the dosage to 8.0 g L^{-1} and keeping the initial DB2 concentration and particle size range of the previous design. Under these optimized conditions a maximum adsorption capacity of 158.085, 132.043 and 101.841 mg g^{-1} at 298, 308, and 318 K was respectively obtained. The evaluation of the kinetics showed the best adjustment with the Elovich equation at 298 and 308 K with a correlation coefficient R^2 = 0.95 and 0.97 correspondingly, whereas at 318 K the second-order model exhibited the best fit with a R^2 = 0.97. Regarding process equilibrium, the Langmuir-Freundlich equation was found to present the best fit over the four evaluated models with an average adjustment coefficient R^2 = 0.99. Further, the assessment of the R_L value in a concentration range of 5–4,000 ppm for all temperatures led to values between 0 and 1.0 which support the favorability of this adsorption process. Finally, the thermodynamic parameters with negative values for Gibbs free energy (ΔG = –1,435.41 J mol^{-1}) and enthalpy (ΔH = –14,813.54 J mol^{-1}) pointed out the spontaneity and exothermic feature of the process, while entropy described a slight randomness at the interface of the solution (ΔS = –44.87 J mol^{-1} K^{-1}). Thus, the obtained results suggest CC as a novel and promising adsorbent for a feasible scaling up of this process.

Keywords: Dye-bearing effluents; Adsorption; Agricultural by-product; Kinetic equilibrium and thermodynamic; Design of experiments

1. Introduction

The presence of synthetic dyes in rivers and lakes represents a serious and recurring environmental issue in Colombia, which is mainly attributed to the textile and food industries that currently discharge their liquid effluents without any prior treatment. In the case of the textile industry with its multiple unit operations and due to the use of different raw materials, reagents and production methods, the discharges contain residues of salts, starch, peroxides, surfactants, metals, emulsifiers and dyes, among others.

Particularly, the aromatic structure of the dyes explains their high resistance to light, heat, and weather conditions with the subsequent slow and difficult degradation that turns the dye-bearing effluents into real sources of pollution. Their presence, even at concentrations less than 1 ppm [1], affects gas solubility, water transparency, and

* Corresponding author.

the habitat aesthetics. Likewise, these molecules increase both the biochemical oxygen demand and the chemical oxygen demand, and lead to a decrease in the entry of sunlight, interrupting the photosynthetic process. This fact promotes anoxic conditions which are highly harmful to the aquatic biota [1–5]. Furthermore, the recalcitrant nature of dyes can cause cytotoxic and genotoxic effects, triggering allergic reactions and genome damage [6–8].

There are different methods to treat dissolved dyes and organic matter contained in water, such as treatment with manganese nanoparticles that have photo-catalytic effects on their degradation [9] or recent technologies such as combined electrocoagulation with bio adsorption where removals of up to 90.01% were obtained [10]. On the other hand, the concern about the environment and natural resources has given rise to a critical view on the suitability of the methods to be used for dissolved pollutant treatment, such as synthetic dyes. In this sense, adsorption may be promising for removing this type of pollutants and other organic matter dissolved in wastewaters. Several materials, including clay materials, such as halloysite [11], cobalt-doped iron [12], or biocomposite with sugarcane bagasse [13] can be used for this process, but natural agricultural by-products has been classified as one of the best alternatives because of its high efficiency, low cost, possible re-use of the adsorbent material, and pollutant retention without molecular breakdown [14,15], avoiding in this way the generation of more toxic compounds, as usually occurs in processes such as photodegradation [16,17].

Regarding the evaluation of agricultural by-products as potential adsorbents, a wide variety is reported, including rice husk, corncob, sugarcane bagasse and coffee husk, among others [18,19]. In our research group, it has been found that corncob is one of the most prominent non-conventional adsorbents, allowing a 99% removal under optimized conditions for both red 40 and tartrazine dyes [20,21]. Moreover, another decisive factor in the group for agricultural by-product selection lies in its wide availability in our environment. In this regard, the Ministry of Agriculture and rural development of Colombia, has reported approximately 1.5 million tons of corn produced in 2018 [22]; a percentage close to 50% corresponds to the grain [23] and the other 50% to the waste such as corncob, leaves and cane, among others. From these residues, it is estimated that corncob represents 18% [24], thus disposing of 135 million tons for the mentioned year. It is worth mentioning that corn is widely spread in regions of the country, given its unique adaptation to diverse agroclimatic and socioeconomic conditions, cultivating two types of corn, yellow and white [25]. In addition, it is valuable to remark that this crop is widespread throughout the world so that the methodology presented here can be replicated anywhere [26].

Concerning synthetic colorants, the Direct blue 2 (DB2) dye is part of the azo compounds, classified as the most prominent chemical group of currently existing dyes (approximately 26,000) [20]. Several studies have shown through animal tests that the azo group is a cause of cancer; therefore, its carcinogenic effect in humans is expected [27]. This dye is widely used in the textile industry and is featured by its large structure consisting of six benzene rings and two azo groups (Fig. 1). An average

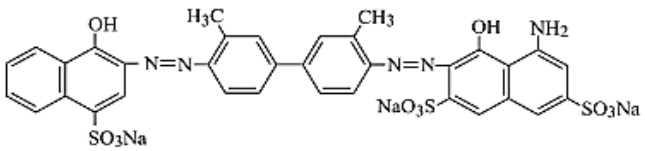

Fig. 1. Direct blue 2 chemical structure [24].

percentage close to 15% of non-fixation in the staining process has been reported for these azo dyes in the textile industry [28], indicating that they will be present in industrial wastewaters, disrupting the balance of the surrounding environment.

According to our review on this topic, there are few reported works for DB2 treatment. For instance, Hashem [29] showed the removal of DB2 with modified wood pulp, adsorbent that is obtained not from a residue but from a material with other possible applications and for whose preparation, the addition of different organic bases such as dimethylamine and epichloridrine is required through a prolonged stirring and heating reaction that definitely makes the process unfeasible. The use of coal obtained from banana peel is proposed by Peluffo and Castro [30] for the retention of DB2, reporting efficiencies between 70 and 80%, results that, although satisfactory, are derivate from the application of a univariate study model. Besides, this alternative implies additional energy costs to carbonize this agricultural by-product. Also, coffee waste is reported for the adsorption of DB2 under continuous process [31] and it should be mentioned that this study considered very small ranges for the selected variables that do not guarantee optimal results for a possible scale-up of the process.

The previous overview points out that corncob (CC) has not yet been evaluated as a potential and unconventional adsorbent in the removal of the azo dye DB2. Therefore, in the present work two objectives were set, firstly, to evaluate the removal capacity of CC in the retention of the DB2 dye until process optimization and secondly, to carry out the study of kinetics, equilibrium and thermodynamics of this process with the overall purpose to establish the possible use of this agricultural waste for a subsequent scaling up of this process. For the study of kinetics, the Elovich, pseudo-first and pseudo-second-order equations were considered, while for the equilibrium evaluation the Langmuir, Freundlich, Langmuir-Freundlich and Redlich-Peterson models were selected. The spontaneity of the process was defined with the thermodynamic parameters of free energy, enthalpy and entropy. In addition, it should be noted that to guarantee the reliability of the results, a factorial design with replications of three units were carried out in each assay.

2. Materials and methods

2.1. Preparation of DB2 solution

The commercial Direct blue 2, whose color index corresponds to CI 22590 was purchased with 98% purity from the company Colorquimica S.A. (Medellín, Colombia). This direct dye with a double azo group has a molecular formula $C_{32}H_{21}N_6Na_3O_{11}S_3$, a molar mass of 830.71 g mol^{-1} and is widely used in the textile industry (Fig. 1). The other

chemical reagents, sodium hydroxide and hydrochloric acid 37%, were purchased at Sigma-Aldrich (Mexico).

A standard solution of 120 mg L^{-1} DB2 dye was prepared in deionized water, from which dilutions to make the respective calibration curve were performed, and the absorbance was measured at the maximum wavelength of this dye, λ_{max} = 562 nm.

2.2. Agricultural by-product pretreatment

The agricultural by-product corncob (CC) was obtained from a local market in Medellín (Colombia) and was subjected to a milling and sieving process to obtain a particle size between 300–1,000 μm. These particles were then washed five times with deionized water to eliminate a slightly yellow color, dried at 60°C for 48 h in a forced convection oven, and finally stored in airtight containers for subsequent adsorption tests.

2.3. DB2 adsorption through factorial and response surface designs with a central point

The adsorption process was performed under a discontinuous system using for each test 25 mL of the dye solution in 25 mL Erlenmeyer flasks. Once the respective contact time was over, the dyed material was separated from the residual solution by filtration. To calculate the removal capacity, the absorbances of the starting and remaining solutions were measured with a Perkin Elmer UV-Vis Lambda 35 spectrophotometer (Mexico) at the maximum absorption wavelength of this dye. The response variable, percentage of DB2 removal (% Rem.), was calculated using Eq. (1) presented in Hashem [29].

First, a 2^3 full factorial design with a central point was carried out to evaluate the following factors, adsorbent dosage (*D*), initial dye concentration (Co) and particle size (Ps), whose levels are detailed in Table 1. All measurements were performed in triplicate for statistical support; each test had three replicates for a total of 27 samples. The fixed conditions for this experiment included a pH = 2.0, which was adjusted with the addition of 1.0 N solutions of NaOH and HCl, stirring speed of 180 rpm, contact time of 2 days at room temperature, these values correspond to the most appropriate conditions from previous tests. After the required time, an aliquot was taken, centrifuged at 180 rpm, and the concentration of the dye was measured in the supernatant. Subsequently, to achieve optimal conditions for DB2 removal onto corncob, a response surface design with a central point was carried out, bearing in mind the most influential factors of the previous factorial design, which were *D* and Co. The ranges taken for this experiment are detailed in Table 1. Similarly, each test was carried out in triplicate for a total of 27 samples. Statistical tests were assessed with 95% confidence. Analysis of variance (ANOVA) was used for comparing results. Besides, to ensure independence, samples were selected, and treatments were applied at random.

2.4. Evaluation of DB2 adsorption kinetics

The adsorption kinetics allows to determine how quickly the dye interacts with the adsorbent surface, being one of the most important characteristics that define the efficiency of an adsorbent. In this work, three kinetic equations corresponding to the kinetics of pseudo-first-order, pseudo-second-order and Elovich were implemented by the study of Azizian [32].

2.5. Pseudo-first-order

It is one of the most widely used kinetic models that can be mathematically expressed as Eq. (1) [33,34].

$$\ln\left(\frac{q_e}{q_e - q_t}\right) = -K_1 t \tag{1}$$

where q_e and q_t are the amount of adsorbate transferred to the surface of the adsorbent at equilibrium and time *t*, respectively, K_1 is the speed constant in min^{-1} and can be calculated from the slope by plotting $\ln(q_e/q_e - q_t)$ vs. *t*.

2.6. Pseudo-second-order equation

This model is based on the adsorption capacity in equilibrium and assumes that the adsorption speed is directly proportional to the square of available sites; it is mathematically expressed as Eq. (2) [35,36].

$$\frac{t}{q_t} = \frac{1}{K_2 q_e^2} + \frac{1}{q_e} t \tag{2}$$

where q_t is the amount of adsorbed dye on the surface of the adsorbent in a certain time (mg g^{-1}), *t* is the time (min), q_e is the amount of adsorbate on the surface of the

Table 1
Factors and levels of the 2^3 full factorial and the central composite response surface design for DB2 removal

Factors	2^3 factorial design			Surface design		
	Levels			Levels		
	(–1)	Central	(+1)	(–1)	Central	(+1)
Adsorbent dosage *D* (g L^{-1})	2.0	4.0	6.0	4.0	5.0	8.0
Initial concentration Co (ppm)	60	150	240	60	150	240
Particle size Ps (mm)	0.3–0.5	0.5–0.7	0.7–1.0	–	–	–

adsorbent at equilibrium (mg g^{-1}), and K_2 is the speed constant (g mg^{-1} min^{-1}). By plotting t/q_t vs. t, the value of the constant from the intercept can be calculated.

2.7. Elovich equation

This model assumes that the active sites of the adsorbent are heterogeneous and therefore exhibit different activation energies that are represented as follows in Eq. (3) [36].

$$q_t = \frac{\ln(\beta\alpha)}{\beta} + \frac{1}{\beta}\ln(t) \tag{3}$$

where α is the initial adsorption rate (mg g^{-1} min^{-1}) and β is the activation energy by chemo-absorption (mg g^{-1}). By plotting q_t vs. ln(t), α and β can be calculated from the slope and intercept.

2.8. Evaluation of the kinetics of the process

To evaluate the DB2 kinetics, the solution was prepared according to the best conditions obtained from the optimization with the surface design, a dosage of 8.0 g L^{-1} and an initial dye concentration of 60 ppm. In 100 mL Erlenmeyer flasks, 20 mL of the solution was taken for each assay. These Erlenmeyer were sealed and placed in a shaker with an incubator to keep the temperature constant throughout the process at a stirring speed of 180 rpm. These solutions were monitored for 12 h with sampling times of 1, 2, 4, 6, 8, 10, 15, 20, 30, 60, 90, 120, 180, 420, and 720 min.

These samples were measured at the maximum absorption wavelength to determine the residual dye concentration. All analyzes were performed in triplicate way at temperatures of 298, 308, 318, and 328 K. Subsequently, Eqs. (1)–(3) were used to determine the model that best fits the experimental results.

2.9. Evaluation of DB2 equilibrium

Adsorption isotherms are essential for describing the interaction between the dye and the adsorbent and very useful to determine the adsorbent capacity of different materials. In particular, Langmuir, Freundlich, Langmuir-Freundlich, and Redlich-Peterson mathematical models were implemented in this work [37,38]. All analyzes were performed in triplicate way at temperatures of 298, 308, 318, and 328 K.

2.10. Langmuir model

The Langmuir isotherm is a theoretical model suitable for adsorption in a monolayer on a completely homogeneous surface with a finite number of identical and specific adsorption sites so that only one molecule is retained or linked to each other; therefore, an interaction between the molecules is negligible. The corresponding equation is mathematically expressed as follows [38].

$$q_e = Q_{\max}\frac{K_L C_e}{1 + K_L C_e} \tag{4}$$

where $Q_{\max}$ is the maximum capacity of the adsorbate under given conditions, in this case DB2 (mg g^{-1}), K_L is the Langmuir constant indicating the affinity of the adsorbate for the adsorbent, q_e is the amount of adsorbate transferred to the surface of the adsorbent, and C_e is the concentration of the adsorbate in equilibrium.

2.11. Freundlich model

Freundlich equation in contrast to Langmuir model considers that the surface of the adsorbent is heterogeneous, and adsorption positions have different affinities, occupying first those of greater affinity and then the others [39,40]. This model is described as follows by Eq. (5).

$$q_e = K_F C_e^{1/n} \tag{5}$$

where K_F is the Freundlich constant associated with the adsorption capacity of the dye, n is the Freundlich constant indicating the intensity of the adsorption, q_e is the amount of adsorbate transferred to the surface of the adsorbent, and C_e is the concentration of the adsorbate in the equilibrium.

2.12. Langmuir-Freundlich model

This model is used to describe liquid–solid equilibrium systems incorrectly described by the Langmuir model. The mathematical expression of the Langmuir-Freundlich isotherm is as follows [41].

$$q_e = \frac{AC_e^m}{1 + BC_e^m} \tag{6}$$

where A and B are the Langmuir-Freundlich constant in L g^{-1} and L mg^{-1}, respectively, and m is the index of heterogeneity.

2.13. Redlich-Peterson model

This isotherm has a great similarity with the Langmuir-Freundlich model in the sense that it is applied to describe the liquid–solid equilibria when the system is not adequately represented by the Langmuir model. The mathematical expression corresponds to Eq. (7) [42]:

$$q_e = \frac{A'C_e}{1 + B'C_e^g} \tag{7}$$

Standard enthalpy change ($H°$), and standard entropy changes ($S°$) will allow to define the spontaneous or non-spontaneous nature of the selected adsorption process.

2.14. Thermodynamic parameters

Thermodynamic parameters reflect the feasibility of a process. Thus, the evaluation of standard free energy changes (G), standard enthalpy change (H), and standard entropy changes (S) will allow to define the spontaneous or non-spontaneous nature of the selected adsorption process.

To assess these thermodynamic parameters, the method referred by the study of Niwas et al. [43] was used, which

is based on the variation of the thermodynamic equilibrium constant K (or the thermodynamic coefficient) with the change in temperature. The value of K is calculated through the following steps.

First, $K°$ for the adsorption reaction is described as follows:

$$K = \frac{a_s}{a_e} = \frac{v_s C_s}{v_e C_e} \tag{8}$$

where a_s is the activity of the adsorbed solute, a_e is the activity of the solute in solution at equilibrium, C_s is the surface concentration of DB2 in millimoles per gram of exchanger, C_e is the concentration of DB2 at equilibrium (mmol mL^{-1}), v_s is the activity coefficient of the adsorbed solute, and v_e is the activity coefficient of the solute in solution.

When the concentration of the solute in the solution comes to near zero, the activity coefficient approaches unity, reducing (8) and (9).

$$K = \frac{a_s}{a_e} = \frac{C_s}{C_e} \tag{9}$$

Values of $K°$ are obtained by plotting $\ln(C_s/C_e)$ vs. C_s and extrapolating C_s to zero [44]. The straight line obtained is fitted to the points based on a least-squares analysis. Its intercept with the vertical axis gives the values of $K°$. Standard free energy changes (G) for interactions are calculated [45] from Eq. (10).

$$G = -RT\ln(K) \tag{10}$$

where R is the universal gas constant, and T is the temperature in Kelvin.

The enthalpy and entropy are calculated from Eq. (11) by plotting G vs. T, as the intercept and the slope, respectively.

$$G = H - TS \tag{11}$$

3. Results

3.1. Statistical design of experiment

3.1.1. 2^3 full factorial design

Table 2 shows the average removal percentages for each of the 9 experiments, where the first treatment led to the most suitable conditions achieving an efficiency of 88.30% under the highest dosage level (6.0 g L^{-1}) and the lowest level of Co (60 ppm) and Ps (0.3–0.5 mm).

In order to explain this adsorption behavior of the DB2-CC system, the effect of D, Co, and Ps were analyzed by the Pareto chart, where the factors and their interactions are shown from highest to lowest significance (Fig. 2a).

Factors that exceed the vertical line have a statistically significant effect with a confidence level of 95% given by the p-value of the ANOVA analysis (Table 3). The individual interactions are the most significant, and factor D displays a high positive effect on the DB2 removal, which can be explained by the increase of active sites in interaction with dye molecules. On the other hand, an increase in Ps and Co reduce the efficiency of the process, since the surface area is decreased and the number of molecules to be adsorbed is increased, respectively. The foregoing indicates that to improve the removal of DB2 onto CC, Co and Ps must decrease while D must increase. The predictive model for the 2^3 full factorial design is shown in Eq. (12) that yields a maximum removal of 88.95%, with a D of 6.0 g L^{-1}, a Co of 60 mg L^{-1}, and a Ps of 0.3–0.5 mm.

$$\%\text{Rem} = 55.487 + 8.94428D - 0.15731\text{Co} - 31.3776\text{Ps} - 0.00313476D*\text{Co} - 0.700533D*\text{Ps} + 0.03797\text{Co}*\text{Ps} \tag{12}$$

3.1.2. Central composite response surface design

For this analysis, Ps was fixed with the level that led to the best removal of DB2 (0.3–0.5 mm) in the factorial design. For factor D, the range was extended from 2.0 to 8.0 g L^{-1}, as suggested by the previous design. Even though the Pareto chart recommends a decrease in Co, it was decided to set the same range used in the factorial design, since one of the aims of this work is to treat dye-bearing effluents with concentrations greater than 60 ppm in the perspective of removing as much DB2 as possible.

Table 2 shows the removal percentages of the surface design, obtaining in all cases better removals under the set conditions. Again, the conditions of the first experiment led to a maximum removal of 89.81%. With respect to the Pareto chart, a similar behavior to that registered in the factorial design for the individual factors was observed, Fig. 2b; however, the interactions are significant except for the Co-Co interaction (p-values are given in Table 3).

D-Co interaction was positive and D-D was negative, which gives account of the curvatures on the response surface, where the latter being significant reflects a maximum on it, which can be seen in Fig. 2c, pointing out that the selected levels for the design were suitable for the experiment. The surface mapping plot is depicted in Fig. 2d whose mathematical model is given by Eq. (13).

$$\%\text{Rem} = 48.3381 + 14.9691D - 0.316922\text{Co} - 0.988977D^2 + 0.00943D*\text{Co} + 0.000317115C^2 \tag{13}$$

The predictive model, with an adjusted correlation coefficient R^2 = 97.89%, yields a maximum removal of 91.47% at Co of 60 ppm and D of 8.0 g L^{-1}, respectively. Although the increase in efficiency was relatively low, 1.51% experimentally and 2.52% predictively, to those determined in the 2^3 factorial design, these optimal conditions of 60 ppm and 8.0 g L^{-1} were used as the best for the following kinetic and equilibrium experiments, since of the CC is a very low-priced by-product.

3.2. Adsorption kinetics

The experimental data of the adsorption kinetics for the DB2-CC system at temperatures of 298, 308, and 318 K are presented in Figs. 3a–c, respectively at a dosage of 8.0 g L^{-1} and an initial concentration of 60 ppm.

Table 2
Experimental removal percentages for the 2^3 full factorial and central composite surface designs for the DB2-CC system

2^3 factorial design					Surface design			
Co (mg L^{-1})	D (g L^{-1})	Ps (mm)	Rem. %	Desv.	Co (mg L^{-1})	D (g L^{-1})	Rem. %	Desv.
60	6	0.3–0.5	88.30	3.68	60	8	89.81	0.72
60	6	0.7–1.0	68.69	1.00	60	5	84.78	0.39
60	2	0.3–0.5	57.82	5.01	60	2	57.85	4.30
60	2	0.7–1.0	32.76	1.13	150	8	77.68	2.41
150	4	0.5–0.7	38.04	5.78	150	5	65.01	1.70
240	6	0.3–0.5	62.33	2.56	150	2	34.89	4.15
240	6	0.7–1.0	40.10	1.54	240	8	64.78	4.52
240	2	0.3–0.5	26.71	1.46	240	5	50.73	0.22
240	2	0.7–1.0	13.86	2.37	240	2	22.63	1.69

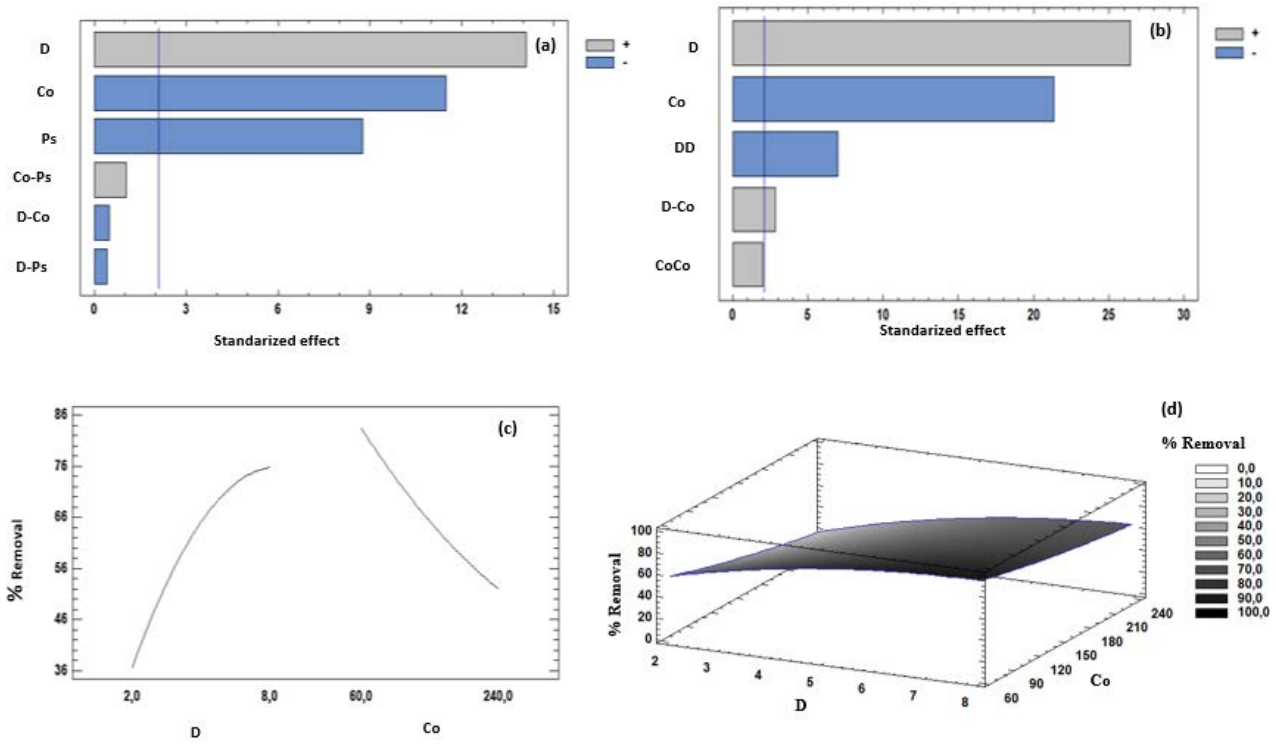

Fig. 2. (a) Pareto chart of the 2^3 full factorial design, (b) Pareto chart of the central composite response surface design, (c) main effects of the central composite response surface design, and (d) 3D surface mapping plot.

As can be seen, the increase in temperature improves the adsorption process, which can be explained by the rise of the molecular speed and the collision against the surface of the adsorbent, leading to a greater amount of adsorbed dye at equilibrium. Nevertheless, the increase of q_t from 298 to 318 K does not exceed 8% according to Table 4, pointing out that 298 K may be a suitable condition for the process and its possible scale-up since, at this temperature, is involved fewer energy costs, at a minimum variation in the adsorbed dye.

In addition, it can be observed that at the beginning of the adsorption, q_t rapidly raises, and after approximately 30 min, the adsorption becomes slower and increases up to 400 min, until finally about 700 min the process approaches to the equilibrium (Fig. 3). The above description allows to differentiate several stages; the first one corresponding to the adsorption of the external or instantaneous surface, where the molecules are directed from the solution to the external surface of the adsorbent; the second, in which the adsorbate diffuses within the pores of the material (intraparticular diffusion) generating a slowdown in the process; until reaching the third stage, the equilibrium, where the net interchange of adsorbate between the liquid and solid support is zero. It can also appreciate that the second and third stages have a small slope that could be fit to a straight line; however, this would not pass through

Table 3
ANOVA *p*-values for the 2^3 full factorial and central composite surface designs for the DB2-CC system

Factors	2^3 factorial design	Surface design
Co	0.0000	0.0000
D	0.0000	0.0000
Ps	0.0000	–
Co-*D*	0.4804	0.0109
Co-Ps	0.1445	–
D-Ps	0.5389	–
Co-*D*-Ps	0.0003	–
Co-Co	–	0.0000
D-*D*	–	0.0585

the origin, which implies that although there is intraparticle diffusion, it is not the only limiting mechanism in the adsorption process, as reported by others authors [46–49].

Table 4 shows the parameters of the evaluated kinetic equations and their corresponding correlations using linear and non-linear regression.

The models that best represent the experimental data according to their correlation coefficient R^2 (non-linear) and the sum of square error, SSE, correspond to Elovich for 298 and 308 K, and pseudo-second-order for 318 K. These equations have also shown a good adjustment with this kind of pollutants [50,51]. It is worth mentioning that the adjustment to Elovich for 298 and 308 K suggests a chemical adsorption process, suitable for heterogeneous adsorption surface systems [52] and similarly, pseudo-second-order at 318 K implies that the limiting step involves a chemisorption where removal occurs by the interaction between the two phases [53].

3.3. Adsorption isotherms

Table 5 summarizes the results of both linear and non-linear adjustment of the equilibrium models with their respective parameters of DB2 adsorption onto CC. It was found that the Langmuir-Freundlich equation presents the best adjustment given by R^2 for the three evaluated temperatures, with a value of 0.997 at 298 K (corresponding to the temperature with the highest capacity at equilibrium), suggesting a monolayer adsorption process [54]. Figs. 4a–c show the experimental data and the model fitting for temperatures of 298, 308, and 318 K, respectively.

Although, the best fit was achieved with the Langmuir-Freundlich equation, Freundlich's model also had a good R^2 and an n value greater than one, suggesting that the adsorption of DB2 onto CC was a chemisorption and a favorable process. On the other hand, the dimensionless parameter, separation factor R_L, characteristic of the Langmuir model [55] is given by Eq. (14).

$$R_L = \frac{1}{1 + K_L C_0} \tag{14}$$

The value of R_L indicates the shape of the isotherm. Unfavorable ($R_L > 1$), linear ($R_L = 1$), favorable ($0 < R_L < 1$) or irreversible ($R_L = 0$) [56]. This factor was evaluated in a

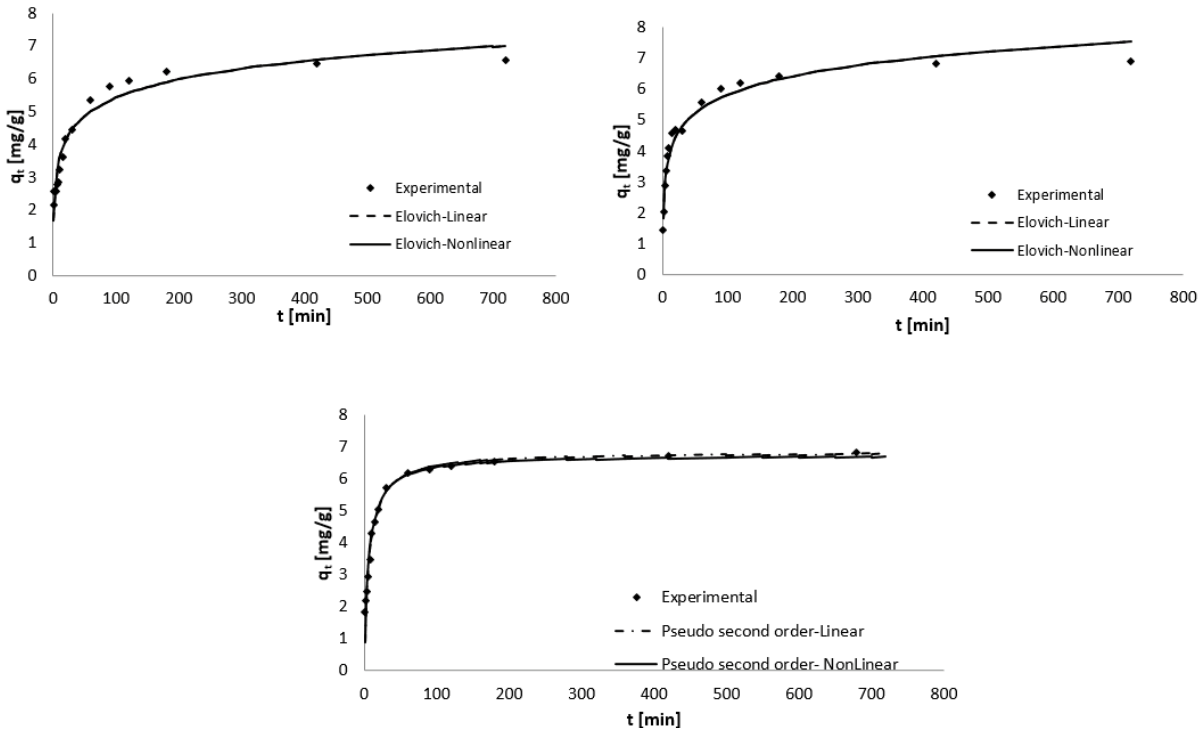

Fig. 3. Adsorption kinetics of DB2 onto CC and adjustments to the models of (a) Elovich at 298 K, (b) Elovich at 308 K, and (c) pseudo-second-order at 318 K.

Table 4
Kinetic parameters for adsorption of DB2 onto CC at different temperatures

Model	Regression	Temperature: 298 K				Temperature: 308 K				Temperature: 318 K			
		K_1 (min^{-1})	q_t (mg g^{-1})	R^2	SSE	K_1 (min^{-1})	q_t (mg g^{-1})	R^2	SSE	K_1 (min^{-1})	q_t (mg g^{-1})	R^2	SSE
Pseudo-first-order	Linear	0.0060	66.328	0.87	2,508	0.0061	69.479	0.88	121.98	0.0067	68.579	0.82	132.88
	Non-linear	0.0860	58.526	0.82	9.37	0.1216	60.156	0.91	5.55	0.1056	63.555	0.95	3.41
		K_2 (g mg^{-1} min^{-1})	q_t (mg g^{-1})			K_2 (g mg^{-1} min^{-1})	q_t (mg g^{-1})			K_2 (g mg^{-1} min^{-1})	q_t (mg g^{-1})		
Pseudo-second-order	Linear	0.0147	66.328	0.84	5.79	0.0154	69.479	0.91	3.64	0.0213	68.579	0.97	1.50
	Non-linear	0.0213	62.283	0.86	5.0	0.0267	64.706	0.96	1.66	0.0235	67.613	0.97	1.43
		B (mg g^{-1} min^{-1}]	α (g mg^{-1} min^{-2})			B (mg g^{-1} min^{-1})	α (g mg^{-1} min^{-2})			B (mg g^{-1} min^{-1})	α (g mg^{-1} min^{-2})		
Elovich	Linear	12.367	65.264	0.95	1.71	11.486	69.130	0.97	1.35	11.240	74.081	0.92	3.81
	Non-linear	12.367	65.263	0.95	1.71	11.486	69.130	0.97	1.35	11.240	74.081	0.92	3.81

concentration range of 5–4,000 ppm for all temperatures, in which values between 0 and 1.0 were obtained, supporting the favorability of this adsorption process.

Moreover, the Redlich-Peterson model represents the second-best fit after Langmuir-Freundlich equation, with an $R^2 > 0.97$ for all three temperatures. This fact suggests that this model, which modifies the Langmuir and Freundlich equations by adding a third parameter, can also adequately represent the DB2-CC system. In particular, a minimum deviation of 0.8% in the Redlich-Peterson R^2 with respect to Langmuir-Freundlich is observed at 318 K.

Table 6 shows the Q_{max} for direct dyes with different agricultural by-products. It is worth mentioning that the CC used in this study has a higher adsorption capacity of DB2 compared to other agricultural by-products such as wheat shells or orange peel. This adsorbent offered even 47.7% higher capacity than the exhibited by activated carbon from orange peel in the adsorption of direct blue N 106 [62] (a compound with some structural similarity to DB2). Thus, CC constitutes a promising adsorbent for the treatment of water polluted with DB2 and probably for other dyes of this chemical nature.

3.4. Thermodynamics

The K values for each temperature were found by plotting $\ln(q_e/C_e)$ vs. q_e and extrapolating q_e to zero [43]. The plots obtained are shown in Fig. 5, and the values are given in Table 7 with the other thermodynamic parameters.

Fig. 6 shows the experimental points of the isotherms and how the increase in temperature leads to a lower process efficiency since the amount of adsorbed dye decreases.

This behavior can be verified with the negative values obtained for enthalpy (Table 7), which point out that the process is exothermic and favorable, and may even occur at lower temperatures than those evaluated. On the other hand, the negative values of Gibbs free energy prove the spontaneous and feasible nature of the process where, at higher temperatures, the energy released is less, denoting the greater feasibility of the process at lower temperatures. The negative entropy found at the evaluated temperatures can be explained due to a decrease in randomness at the solution-solid interface during the DB2 adsorption onto CC. Despite the fact that this parameter is unfavorable, its value is relatively small, so that it does not affect the overall spontaneity of the process [66]. It is worth noting that the value of entropy and enthalpy for the three evaluated temperatures is the same, since according to the used calculation method, these parameters are considered as characteristic properties of each reaction that do not change with temperature as occurs with the Gibbs free energy [43].

4. Conclusions

In this work, for the first time the CC agricultural by-product was evaluated as an alternative and novel adsorbent for the treatment of polluted effluents with DB2 dye. A 2^3 full factorial design was performed to establish the best conditions of the adsorption process of this dye. It was found that CC owns a high adsorption capacity for the DB2 dye removal, reaching 88.3% efficiency under a dosage of 6.0 g L^{-1}, a dye concentration of 60 ppm, and a particle

Table 5
Parameters of adsorption isotherms of DB2 onto CC at different temperatures

		Temperature: 298 K				Temperature: 308 K				Temperature: 318 K			
Model	Regression	Q_{max}	K_L	R^2	–	Q_{max}	K_L	R^2	–	Q_{max}	K_L	R^2	–
Langmuir	Linear	148.545	0.005	0.944	–	123.221	0.006	0.936	–	98.426	0.012	0.936	–
	Non-linear	158.085	0.002	0.982	–	132.043	0.003	0.972	–	101.841	0.007	0.969	–
		K_F	n	R^2	–	K_F	n	R^2	–	K_F	n	R^2	–
Freundlich	Linear	2.696	1.874	0.912	–	5.208	2.386	0.967	–	7.896	2.942	0.949	–
	Non-linear	6.206	2.499	0.995	–	7.373	2.749	0.982	–	10.975	3.464	0.965	–
		A	B	m	R^2	A	B	m	R^2	A	B	m	R^2
Langmuir-Freundlich	Non-linear	4.777	0.009	0.471	0.997	3.711	0.017	0.551	0.989	4.046	0.031	0.598	0.985
		A'	B'	g	R^2	A'	B'	g	R^2	A'	B'	g	R^2
Redlich-Peterson	Linear	0.541	0.279	0.418	0.905	20.000	4.879	0.545	0.945	1.537	0.248	0.622	0.865
	Non-linear	5.312	0.667	0.631	0.997	20.291	2.539	0.647	0.983	1.537	0.052	0.839	0.977

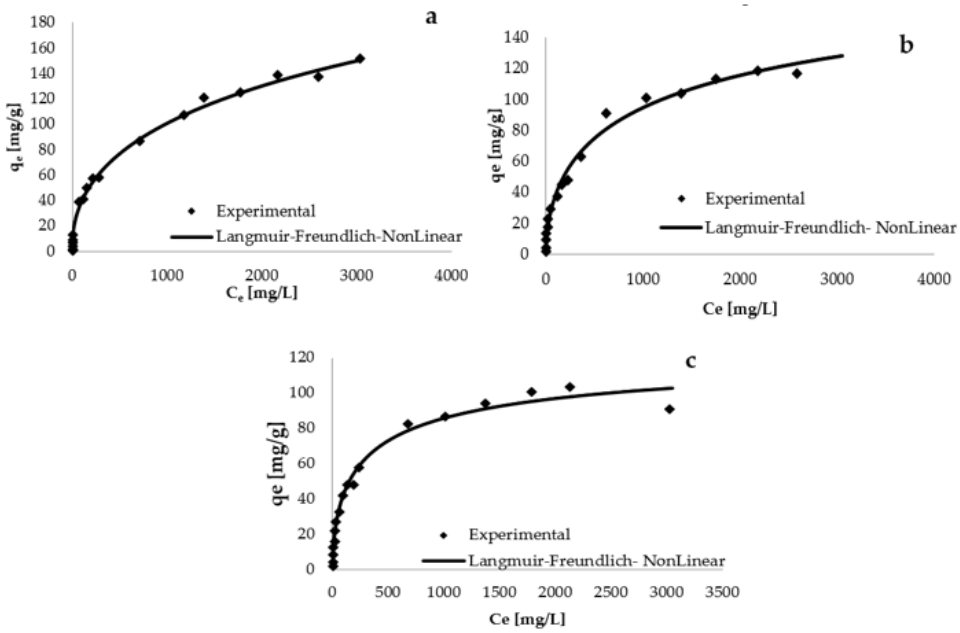

Fig. 4. DB2-CC adsorption equilibrium and adjustments to the Langmuir-Freundlich model at temperatures of (a) 298 K, (b) 308 K, and (c) 318 K.

size range of 0.3–0-5 mm. In order to optimize the process, a subsequent central composite response surface design was performed obtaining a maximum DB2 dye removal of 89.81% at 60 ppm and 8.0 g L^{-1} and fixing the initial DB2 concentration and the particle size of the previous design. These findings pointed out that the increase in the adsorbent dosage did not improve the process, since the percentage of efficiency had a minimal increase. In this way, the removal of DB2 could be carried out satisfactorily using a smaller amount of adsorbent, which would allow to reduce the costs of the process. Under the optimal conditions, the maximum adsorption capacity obtained at 298, 308, and 318 K was 158.085, 132.043 and 101.841 mg g^{-1} respectively, values higher than which reported for others agricultural by-products such as wheat shells or orange peel.

Regarding the evaluation of adsorption kinetics of DB2 onto CC, the Elovich model showed the best description of the process at temperatures of 298 and 308 K, while at 318 K the pseudo-second-order equation offered the best fit. In the case of equilibrium, the Langmuir-Freundlich model corresponded to the best fit for the three evaluated temperatures, suggesting a monolayer process, with adsorption of a chemical nature. Furthermore, and in accordance with the values found for Gibbs free energy and enthalpy, the removal process of DB2 dye is spontaneous and exothermic respectively (G = –1435.41 J mol^{-1}

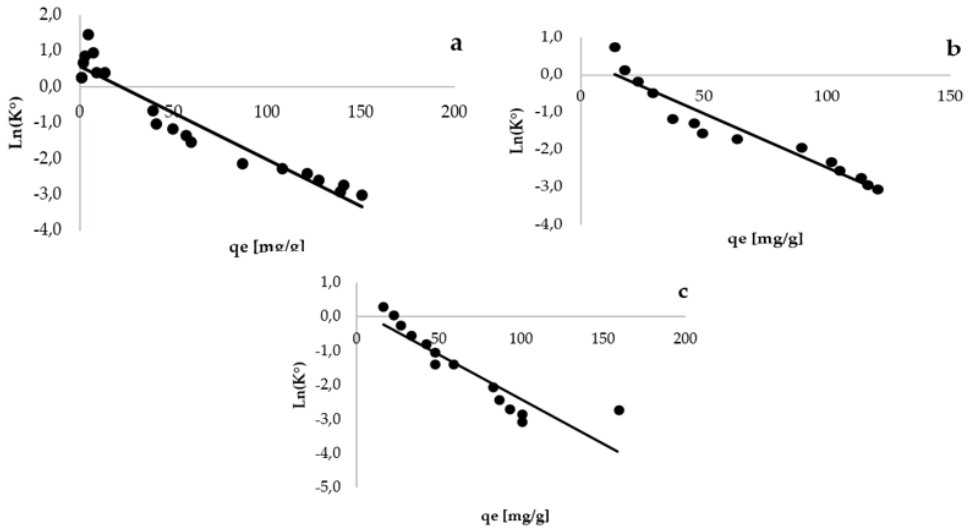

Fig. 5. Plot of $\ln(q_e/C_e)$ vs. qe for at (a) 298 K, (b) 308 K, and (c) 318 K.

Table 6
Maximum adsorption capacity of direct dyes on agro-industrial adsorbents

Adsorbent	Dye	Q_{max} (mg g^{-1})	Reference
Compost	Direct blue 71	22	[57]
Compost	Direct orange 39	17	[57]
Almond shells	Direct red 80	22.4	[58]
Orange peel	Direct red 23	10.7	[59]
Orange peel	Direct red 80	21.1	[59]
Soy meal hull	Direct red 80	178.6	[60]
Soy meal hull	Direct red 81	120.5	[60]
Fe(III)/Cr(III) hydroxide	Direct red 12B	5.0	[61]
Activated carbon from orange peel	Direct blue 86	33.78	[62]
Activated carbon from orange peel	Direct N blue 106	107	[63]
Banana pith	Direct red	5.92	[64]
Activated carbon from pomegranate peel	Direct blue 106	42.59	[51]
Wheat shells	Direct blue 71	40.82	[65]
Corncob	Direct blue 2	158.085 (298 K)	This study
		132.043 (308 K)	
		101.841 (318 K)	

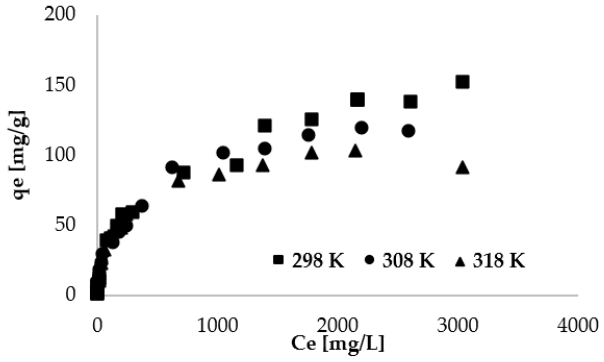

Fig. 6. Experimental points of adsorption isotherms.

and H = –14,813.54 J mol^{-1}). Entropy showed a negative value corresponding to a slight randomness at the interface of the solution (S = –44.87 J mol^{-1} K^{-1})

Finally, the great uptake capacity in the DB2 removal onto CC, together with the favorable conditions of the process, defined by the thermodynamic parameters, and the findings of the equilibrium and kinetics, allow suggesting the feasibility of a posterior study of the process under continuous system with the future expectation of scaling up the process in order to contribute for solving the problem of treating effluents with persistent pollutants.

Acknowledgments

The authors express thanks to the Universidad Nacional de Colombia – Sede Medellín for the financial

Table 7
Thermodynamic parameters

Temperature (K)	K	H (J mol^{-1})	S (J mol^{-1} K^{-1})	G (J mol^{-1})
298	1.77	–14,813.54	–44.87	–1,435.41
308	1.49	–14,813.54	–44.87	–986.70
318	1.22	–14,813.54	–44.87	–538.00

support, as well as for the infrastructure of the Experimental Chemistry Laboratory.

References

[1] F.A. Amaringo, F. Alberto, A. del Socorro, Adsorption of red 40 dye on rice husk: determination of the equilibrium, kinetic and thermodynamic of the process, Tecnura, 22 (2018) 13–28.
[2] G.E. Walsh, L.H. Bahner, W.B. Horning, Toxicity of textile mill effluents to freshwater and estuarine algae, crustaceans and fishes, Environ. Pollut. Ser. A, 21 (1980) 169–179.
[3] D. Brown, Effects of colorants in the aquatic environment, Ecotoxicol. Environ. Saf., 13 (1987) 139–147.
[4] K.T. Chung, C.E. Cerniglia, Mutagenicity of azo dyes: structure-activity relationships, Mutat. Res., 277 (1992) 201–220.
[5] G. de Aragão Umbuzeiro, H.S. Freeman, S.H. Warren, D.P. de Oliveira, Y. Terao, T. Watanabe, L.D. Claxton, The contribution of azo dyes to the mutagenic activity of the Cristais River, Chemosphere, 60 (2005) 55–64.
[6] H. Moawad, W.M. Abd El-Rahim, M. Khalafallah, Evaluation of biotoxicity of textile dyes using two bioassays, J. Basic Microbiol., 43 (2003) 218–229.
[7] P.A. Carneiro, G.A. Umbuzeiro, D.P. Oliveira, M.V.B. Zanoni, Assessment of water contamination caused by a mutagenic textile effluent/dyehouse effluent bearing disperse dyes, J. Hazard. Mater., 174 (2010) 694–699.
[8] D.S. Brookstein, Factors associated with textile pattern dermatitis caused by contact allergy to dyes, finishes, foams, and preservatives, Dermatol. Clin., 27 (2009) 309–322.
[9] U. Kamran, H.N. Bhatti, M. Iqbal, S. Jamil, M. Zahid, Biogenic synthesis, characterization and investigation of photocatalytic and antimicrobial activity of manganese nanoparticles synthesized from *Cinnamomum verum* bark extract, J. Mol. Struct., 1179 (2019) 532–539.
[10] F. Javed, S.W. Ahmad, A. Ikhlaq, A. Rehman, F. Saleem, Elimination of basic blue 9 by electrocoagulation coupled with pelletized natural dead leaves (*Sapindus mukorossi*) biosorption, Int. J. Phytorem., 23 (2021) 462–473.
[11] I. Anastopoulos, A. Mittal, M. Usman, J. Mittal, G.H. Yu, A. Núñez-Delgado, M. Kornaros, A review on halloysite-based adsorbents to remove pollutants in water and wastewater, J. Mol. Liq., 269 (2018) 855–868.
[12] S. Soni, P.K. Bajpai, J. Mittal, C. Arora, Utilisation of cobalt doped Iron based MOF for enhanced removal and recovery of methylene blue dye from waste water, J. Mol. Liq., 314 (2020) 113642, doi: 10.1016/j.molliq.2020.113642.
[13] S. Noreen, H.N. Bhatti, M. Iqbal, F. Hussain, F.M. Sarim, Chitosan, starch, polyaniline and polypyrrole biocomposite with sugarcane bagasse for the efficient removal of Acid Black dye, Int. J. Biol. Macromol., 147 (2020) 439–452.
[14] H. Singh, G. Chauhan, A.K. Jain, S.K. Sharma, Adsorptive potential of agricultural wastes for removal of dyes from aqueous solutions, J. Environ. Chem. Eng., 5 (2017) 122–135.
[15] L. Pereira, M. Alves, Dyes—Environmental Impact and Remediation, A. Malik, E. Grohmann, Eds., Environmental Protection Strategies for Sustainable Development, Springer, Dordrecht, 2012, pp. 111–162.
[16] F. Gosetti, U. Chiuminatto, E. Mazzucco, G. Calabrese, M.C. Gennaro, E. Marengo, Identification of photodegradation products of Allura Red AC (E129) in a beverage by ultra high-performance liquid chromatography–quadrupole-time-of-flight mass spectrometry, Anal. Chim. Acta, 746 (2012) 84–89.
[17] M.M. Sousa, C. Miguel, I. Rodrigues, A.J. Parola, F. Pina, J.S. Seixas de Melo, M.J. Melo, A photochemical study on the blue dye indigo: from solution to ancient Andean textiles, Photochem. Photobiol. Sci., 7 (2008) 1353–1359.
[18] V.K. Gupta, Suhas, Application of low-cost adsorbents for dye removal – a review, J. Environ. Manage., 90 (2009) 2313–2342.
[19] G. Crini, Non-conventional low-cost adsorbents for dye removal: a review, Bioresour. Technol., 97 (2006) 1061–1085.
[20] A. Hormaza, D. Figueroa, A. Moreno, Evaluation of the removal of an azo dye on corncob by statistical design, Rev. Fac. Cienc., 1 (2012) 61–71.
[21] A. Moreno, D. Figueroa, A. Hormaza, Statistical design for the efficient removal of red dye 40 on corncob, P + L, 7 (2012) 9–19.
[22] Corn, Directorate of Agricultural and Forestry Chains, Department of Agriculture, April 2019. Available at: https://sioc.minagricultura.gov.co/AlimentosBalanceados/Documentos/2019-03-30%20Cifras%20Sectoriales%20Ma%C3%ADz.pdf (accessed on 27 May 2020).
[23] L.V. Peñaranda, S.P. Montenegro, P.A. Girardo, Use of agroindustrial waste in Colombia, RIAA, 8 (2017) 141–150.
[24] C. Berrastegui, J.P. Ortega, J.M. Mendoza, Y.E. Gonzáles, R.D. Gómez, Manufacture of densified solid biofuels from corncob, cassava biofuel and mineral coal from the department of Córdoba, Ingeniare. Rev. Chil. Ing., 25 (2017) 643–653.
[25] M.G. Polonia, Technical Aspects of Corn Production in Colombia: Importance of Corn Growing, FENALCE, 2014.
[26] B. Leff, N. Ramankutty, J.A. Foley, Geographic distribution of major crops across the world, Global Biogeochem. Cycles, 18 (2004), doi: 10.1029/2003GB002108.
[27] V.K. Balakrishnan, S. Shirin, A.M. Aman, S.R. de Solla, J. Mathieu-Denoncourt, V.S. Langlois, Genotoxic and carcinogenic products arising from reductive transformations of the azo dye, Disperse Yellow 7, Chemosphere, 146 (2016) 206–215.
[28] C. O'Neill, F.R. Hawkes, D.L. Hawkes, N.D. Lourenço, H.M. Pinheiro, W. Delée, Colour in textile effluents – sources, measurement, discharge consents and simulation: a review, J. Chem. Technol. Biotechnol., 74 (1999) 1009–1018.
[29] A. Hashem, Preparation of a new adsorbent based on wood pulp for the removal of Direct Blue 2 from aqueous solutions, Polym. Plast. Technol. Eng., 45 (2006) 779–783.
[30] G.A. Peluffo, S. Castro, Evaluation of the Adsorption Capacity of Direct Navy Blue Dye (AMD) in Aqueous Solution with Carbon Obtained from Banana Peels, Dis. Universidad de la Costa, 2019.
[31] G.C. Castelar, M.M. Cely, B.M. Cardozo, E.R. Angulo, M.E. Plaza, Adsorption of direct blue dye 2 on coffee grounds in a laboratory scale fixed bed column, Revista UDCA Actualidad & Divulgación Científica, 21 (2018) 531–541.
[32] S. Azizian, Kinetic models of sorption: a theoretical analysis, J. Colloid Interface Sci., 276 (2004) 47–52.
[33] N.M. Mahmoodi, U. Sadeghi, A. Maleki, B. Hayati, F. Najafi, Synthesis of cationic polymeric adsorbent and dye removal isotherm, kinetic and thermodynamic, J. Ind. Eng. Chem., 20 (2014) 2745–2753.
[34] S.J. Allen, Q. Gan, R. Matthews, P.A. Johnson, Kinetic modeling of the adsorption of basic dyes by kudzu, J. Colloid Interface Sci., 286 (2005) 101–109.
[35] Y.S. Ho, Review of second-order models for adsorption systems, J. Hazard. Mater., 136 (2006) 681–689.
[36] N. Yeddou, A. Bensmaili, Kinetic models for the sorption of dye from aqueous solution by clay-wood sawdust mixture, Desalination, 185 (2005) 499–508.
[37] Z. Aksu, U. Açikel, E. Kabasakal, S. Tezer, Equilibrium modelling of individual and simultaneous biosorption of chromium(VI) and nickel(II) onto dried activated sludge, Water Res., 36 (2002) 3063–3073.

[38] P.C.C. Faria, J.J.M. Orfão, M.F.R. Pereira, Adsorption of anionic and cationic dyes on activated carbons with different surface chemistries, Water Res., 38 (2004) 2043–2052.
[39] A. Ahmad, A. Idris, D.K. Mahmoud, Equilibrium modeling, kinetic and thermodynamic studies on the adsorption of basic dye by low-cost adsorbent, J. Adv. Res. Sci. Eng. Technol., 1 (2011) 261–277.
[40] Z. Aksu, A.İ. Tatlı, Ö. Tunç, A comparative adsorption/biosorption study of Acid Blue 161: effect of temperature on equilibrium and kinetic parameters, Chem. Eng. J., 142 (2008) 23–39.
[41] J.C. Bellot, J.S. Condoret, Modelling of liquid chromatography equilibria, Process Biochem., 28 (1993) 365–376.
[42] K.Y. Foo, B.H. Hameed, Insights into the modeling of adsorption isotherm systems, Chem. Eng. J., 156 (2010) 2–10.
[43] R. Niwas, U. Gupta, A.A. Khan, K.G. Varshney, The adsorption of phosphamidon on the surface of styrene supported zirconium(IV) tungstophosphate: a thermodynamic study, Colloids Surf., A, 164 (2000) 115–119.
[44] J.W. Bigar, M.W. Cheung, Adsorption of picloram (4-amino-3,5,6-trichloropicolinic acid) on panoche, ephrata, and palouse soils: a thermodynamic approach to the adsorption mechanism, Soil Sci. Soc. Am. J., 37 (1973) 863–868.
[45] S. Glasstone, Textbook of Physical Chemistry, Macmillan, 1951.
[46] A. Safa Özcan ,Ş. Tetik, A. Özcan, Adsorption of acid dyes from aqueous solutions onto sepiolite, Sep. Sci. Technol., 39 (2004) 301–320.
[47] A. Özcan, A.S. Özcan, Adsorption of Acid Red 57 from aqueous solutions onto surfactant-modified sepiolite, J. Hazard. Mater., 125 (2005) 252–259.
[48] R.P. Han, J.J. Zhang, P. Han, Y.F. Wang, Z.H. Zhao, M.S. Tang, Study of equilibrium, kinetic and thermodynamic parameters about methylene blue adsorption onto natural zeolite, Chem. Eng. J., 145 (2009) 496–504.
[49] Y.S. Murillo, L. Giraldo, J.C. Moreno, Determinación de la cinética de adsorción de 2, 4-dinitrofenol en carbonizado de hueso bovino por espectrofotometría uv-vis, Rev. Colomb. de Química, 40 (2011) 91–103.
[50] A. Hashem, F. Ahmad, S.M. Badawy, Adsorption of direct green 26 onto fix 3500 treated sawdust: equilibrium, kinetic and isotherms, Desal. Water Treat., 57 (2016) 13334–13346.
[51] N.K. Amin, Removal of direct blue-106 dye from aqueous solution using new activated carbons developed from pomegranate peel: adsorption equilibrium and kinetics, J. Hazard. Mater., 165 (2009) 52–62.
[52] F.-C. Wu, R.-L. Tseng, R.-S. Juang, Characteristics of Elovich equation used for the analysis of adsorption kinetics in dye-chitosan systems, Chem. Eng. J., 150 (2009) 366–373.
[53] D. Robati, Pseudo-second-order kinetic equations for modeling adsorption systems for removal of lead ions using multi-walled carbon nanotube, J. Nanostruct. Chem., 3 (2013) 55, doi: 10.1186/2193-8865-3-55.
[54] J. Mieczysław, A. Deryło, A. Marczewski, The Langmuir-Freundlich equation in adsorption from dilute solutions on solids, Monatsh. Chem., 114 (1983) 393–397.
[55] T.W. Weber, R.K. Chakravorti, Pore and solid diffusion models for fixed-bed adsorbers, AIChE J., 20 (1974) 228–238.
[56] M. Gordon, Adsorption of dyestuffs from aqueous solutions with activated carbon I: equilibrium and batch contact-time studies, J. Chem. Technol. Biotechnol., 32 (1982) 759–772.
[57] L.S. Tsui, W.R. Roy, M.A. Cole, Removal of dissolved textile dyes from wastewater by a compost sorbent, Color. Technol., 119 (2003) 14–18.
[58] F.D. Ardejani, K. Badii, N.Y. Limaee, S.Z. Shafaei, A.R. Mirhabibi, Adsorption of Direct Red 80 dye from aqueous solution onto almond shells: effect of pH, initial concentration and shell type, J. Hazard. Mater., 151 (2008) 730–737.
[59] M. Arami, N.Y. Limaee, N.M. Mahmoodi, N.S. Tabrizi, Removal of dyes from colored textile wastewater by orange peel adsorbent: equilibrium and kinetic studies, J. Colloid Interface Sci., 288 (2005) 371–376.
[60] M. Arami, N.Y. Limaee, N.M. Mahmoodi, N.S. Tabrizi, Equilibrium and kinetics studies for the adsorption of direct and acid dyes from aqueous solution by soy meal hull, J. Hazard. Mater., 135 (2006) 171–179.
[61] C. Namasivayam, S. Sumithra, Removal of direct red 12B and methylene blue from water by adsorption onto Fe(III)/Cr(III) hydroxide, an industrial solid waste, J. Environ. Manage., 74 (2005) 207–215.
[62] A. El Nemr, O. Abdelwahab, A. El-Sikaily, A. Khaled, Removal of direct blue-86 from aqueous solution by new activated carbon developed from orange peel, J. Hazard. Mater., 161 (2009) 102–110.
[63] A. Khaled, A. El Nemr, A. El-Sikaily, O. Abdelwahab, Removal of Direct N Blue-106 from artificial textile dye effluent using activated carbon from orange peel: adsorption isotherm and kinetic studies, J. Hazard. Mater., 165 (2009) 100–110.
[64] C. Namasivayam, D. Prabha, M. Kumutha, Removal of direct red and acid brilliant blue by adsorption on to banana pith, Bioresour. Technol., 64 (1998) 77–79.
[65] Y. Bulut, N. Gözübenli, H. Aydın, Equilibrium and kinetics studies for adsorption of direct blue 71 from aqueous solution by wheat shells, J. Hazard. Mater., 144 (2007) 300–306.
[66] M. Rafatullah, O. Sulaiman, R. Hashim, A. Ahmad, Adsorption of methylene blue on low-cost adsorbents: a review, J. Hazard. Mater., 177 (2010) 70–80.